Scaling of the spanning threshold in gradient percolation

Lincoln Paterson
CSIRO, Private Bag 10, Clayton South, Victoria 3169, Australia
(Received 1 December 2013; revised manuscript received 25 April 2014; published 12 February 2015)

A simple and fast way to apply correlations in percolation simulations is to apply a uniform gradient to the occupancy probabilities. For small networks, exact results are presented here for the spanning thresholds in site percolation with a gradient for networks up to 4×4 in two dimensions and $2 \times 2 \times 2$ in three dimensions. Numerical results are provided for larger networks that extrapolate to a linear modification of the threshold proportional to the gradient for moderate values of the gradient.

DOI: 10.1103/PhysRevE.91.022116 PACS number(s): 64.60.ah, 47.56.+r

I. INTRODUCTION

An important application of percolation theory is to describe multiphase flow in porous media. In this context percolation provides the basis of a theory of one fluid trapping another fluid, particularly the trapping of oil by water. Most of the extensive literature on percolation considers regular networks that are statistically uniform and uncorrelated. However, for the major application of trapping in natural porous media, observations show that most sedimentary rocks are not uniform and correlations exist at all scales down to the pore scale.

To address correlations, significant progress has been made studying percolation on networks constructed using fractional Brownian motion (FBM) [1–7], where these studies are based on observations of FBM-type correlations in field measurements. Nevertheless, an alternative approach to studying correlations in a simple system is the limiting case where the correlations are introduced purely through applying a gradient. As will be shown here, this allows for some exact results on small networks and some straightforward formula for larger networks to be derived. In this work correlations are used in the sense of geostatistics [8], where uncorrelated properties have a constant variogram and correlated properties have a variogram that increases with distance. With a gradient in the network properties, sites near one edge or surface are more likely to be occupied than the opposite edge or surface.

The concept of gradient percolation was first introduced by Sapoval *et al.* [9] and separately for invasion percolation by Wilkinson [10]. Nearly all studies of gradient percolation have been concerned with the fractal geometry of the diffusion front or hull [11–15], although other work has considered conductivity properties [16]. A review of developments in gradient percolation has been provided by Gouyet and Rosso [17]. This paper is different in that the spanning threshold is considered, which includes accounting for sites that are not connected to the hull. The spanning threshold is studied here as it is the quantity most relevant to residual saturation in porous media.

Gradient percolation has particular meaning for flow in porous media where it corresponds to the imposition of buoyancy [10,18]. Furthermore, a gradient in properties has physical meaning for anisotropic rocks that are deposited with upward coarsening (coarsening-up) or upward fining (fining-up) [19]. Upward coarsening and upward fining are often observed by geologists in laboratory core samples where a changing sediment load has created a gradient in grain sizes during deposition. Thus a general understanding of percolation on a gradient is potentially useful. While this study is only concerned with ordinary site percolation, future similar studies could involve more complete flow-network models.

To study percolation with a gradient it is necessary to revisit some definitions. In the usual definition of the ordinary site percolation problem, sites in a lattice have a probability p of being occupied and a corresponding probability $1 - p$ of being unoccupied [20]. The sites are assumed to be statistically equivalent and independent. The percolation threshold p_c is the value of the probability when the lattice first becomes connected. In the approach used by Ziff and Newman [21] to calculate p_c, sites are occupied one by one in random order starting with an empty lattice. For an uncorrelated lattice, this is equivalent to assigning each site a value from a random number generator, then occupying the sites in order, starting at the site with the largest number, and then proceeding progressively toward the smallest number. Similarly to Ziff and Newman [21], the study here is only concerned with the existence or not of a system-spanning cluster, so the simulation is stopped once a spanning cluster is detected, as spanning must occur for all higher values of n. Each simulation then produces a single number, the value of n, denoted by n_c, at which a spanning cluster first appears in a given direction. When averaged over many realizations, the mean of the spanning threshold is denoted by $\langle n_c \rangle$. As the lattice size $L \to \infty$, $\langle n_c \rangle$ converges to p_c. Although this convergence is not the most efficient way to calculate p_c, it is the method used here because it is readily applied to percolation with a gradient.

To apply a gradient in the study described here, the simulations commence with each site being given a random value r generated uniformly over the interval [0,1]. The distance from a chosen edge of the network is then multiplied by a gradient g and added to r, giving values

$$v = r + gi/(L - 1), \tag{1}$$

where i is the row, with i going from 0 to $L - 1$. This means that overall the site values v fall in the interval $[0, 1 + g]$. As described above, the sites are then occupied in order, starting at the site with the largest value of v. To illustrate the concept of percolation with a gradient, examples in two dimensions with $L = 50$ and $g = 0.75$ are shown in Fig. 1 compared to an example with no gradient.

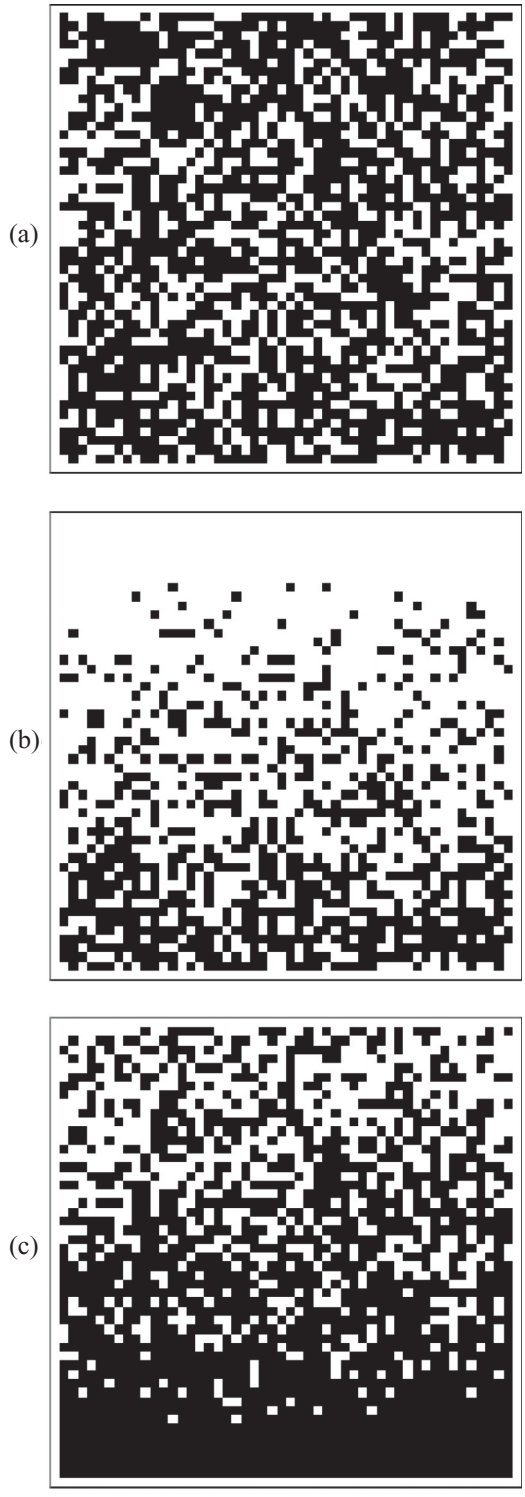

FIG. 1. Examples illustrating percolation on gradient networks: (a) spanning on an uncorrelated network, with $g = 0$; (b) spanning perpendicular to the gradient, with $g = 0.75$; and (c) spanning parallel to the gradient, with $g = 0.75$.

II. EXACT RESULTS IN TWO DIMENSIONS

A. Zero gradient

With $g = 0$ on small $L \times L$ lattices, exact results for the mean spanning fraction in a given direction $\langle n_c \rangle$ can be calculated by considering all possible combinations of ways that sites can be occupied as n goes from 0 to $N = L \times L$ and determining which of these combinations span the lattice. The spanning combinations can be easily extracted using the coefficients in Table III of Ziff and Newman [21]. To illustrate, starting with a 2×2 network in a given direction, there is precisely one way that zero sites can be occupied, four ways that one site can be occupied (with spanning not possible), six ways that two sites can be occupied (with two combinations spanning), four ways that three sites can be occupied (all four spanning), and one way that four sites can be occupied (which must span). Thus the combinations of spanning sites for $n = 0$, 1, 2, 3, and 4 sites occupied can be written (0,0,2,4,1) out of the possible combinations of the ways the sites can be occupied (1,4,6,4,1). Thus the fractions that span for $n = (0,1,2,3,4)$ are given by

$$(0,0,2,4,1)/(1,4,6,4,1) = (0,0,1/3,1,1). \tag{2}$$

This gives the cumulative spanning fraction, so the next step is to take differences to get the spanning frequency for each value of n, with n going from 1 to N (in this case $N = 4$):

$$(0,1/3,1,1) - (0,0,1/3,1) = (0,1/3,2/3,0). \tag{3}$$

The mean spanning fraction $\langle n_c \rangle$ is then given by

$$(0,1/3,2/3,0) \times (1,2,3,4)/4 = 2/3. \tag{4}$$

This calculation can be progressively applied to successive values of L. With $L = 3$ and $N = 9$, the coefficients are

$$(0,0,0,3,22,59,67,36,9,1) \tag{5}$$

and the corresponding binomial sequence is

$$(1,9,36,84,126,126,84,36,9,1), \tag{6}$$

giving

$$\langle n_c \rangle = 116/189. \tag{7}$$

Working through the values of L in Table III of Ziff and Newman [21], this gives the results shown in Table I up to $L = 7$.

TABLE I. Exact results for the site spanning threshold in two dimensions on an uncorrelated lattice with zero gradient ($g = 0$).

L	$\langle n_c \rangle$ exact fraction	$\langle n_c \rangle$ decimal fraction
2	2/3	0.666667
3	116/189	0.613757
4	78527/131040	0.599260
5	1529022307/2574148500	0.593991
6	192290619955183/324907994010600	0.591831
7	233080130675464856 75/3944238459949450 3536	0.590938

B. With a gradient

With a gradient g the combinations with a given number of occupied sites are no longer equiprobable. For instance, when $n = 2$ on a 2×2 lattice, the two combinations that span do not have the same probability. To calculate the probabilities with a gradient, successive site occupancy has to be calculated using the rules of selection without replacement, meaning that all

TABLE II. Exact results for the mean spanning threshold in D dimensions with gradient g, $0 \leqslant g \leqslant 1$.

D	L	$\langle n_{c\perp}\rangle$	$\langle n_{c\parallel}\rangle$
2	2	$(2g^3-3g^2+4)/6$	$(-2g^3+3g^2+8)/12$
2	3	$(93g^7-350g^6-882g^5+3990g^4-5908g^2+9280)/15120$	$(-2g^9+102g^7-840g^6+3591g^5-6468g^4+7128g^2+18560)/30240$
2	4	$(-114048g^{15}+32561352g^{13}-207567360g^{12}+445376516g^{11}-859053195g^{10}+1526382000g^9+7124483223g^8-19335455568g^7-34562814858g^6+80807270544g^5+39511072458g^4-184430694150g^2+306038094318)/510693543360$	$(16686g^{15}+2032020g^{13}-9567558g^{12}+47936018g^{11}-120918798g^{10}-813648264g^9+7591034880g^8-26689455936g^7+46584219825g^6-33946993080g^5-1769573871g^4+19990153215g^2+51006349053)/85115590560$
3	2	$(g^7-28g^5+35g^4+35g^3-56g^2+48)/105$	$(-2g^7-28g^5+35g^4-70g^3+112g^2+128)/280$

occupied sites need to be considered simultaneously for each spanning combination. The possible permutations of spanning combinations rapidly becomes extremely large as L increases, but with some effort, exact solutions for small networks are still possible without enumerating every combination by exploiting exchangeability and symmetry. Here exact solutions up to $L = 4$ are provided in Table II. These formulas for $\langle n_c\rangle$, both perpendicular $\langle n_{c\perp}\rangle$ and parallel $\langle n_{c\parallel}\rangle$ to the gradient, are plotted in Fig. 2. When $g = 0$ these results reduce to the values in Table I. Variances from the mean values $\mathrm{Var}(n_c)$ can also be determined; these are included in Table III with standard deviations plotted in Fig. 3. Again these are different parallel and perpendicular to the gradient.

For finite L when the gradient is extremely large,

$$\langle n_{c\parallel}\rangle = \frac{1}{L}, \quad g \geqslant L. \tag{8}$$

Thus it is possible for sites only along one edge to become occupied. In this study, however, only values $g < 1$ are considered.

III. NUMERICAL RESULTS IN TWO DIMENSIONS

Newman and Ziff [22,23] have developed a very efficient algorithm for studying site or bond percolation on any lattice. Their algorithm uses an amount of time that scales linearly with the size of the system $O(N)$. Their published code was adopted for this study, but with some changes shown in Ref. [24]. Unfortunately, with a gradient, the simulation time is reduced to $O(N \log N)$ rather than $O(N)$ through the need to sort sites.

For the calculations in this paper, the approach of Ziff and Newman [21] is followed using the method where two complete rows of sites at the top and bottom of an open $(L+2)\times(L+2)$ lattice are fixed permanently empty and two columns of L sites on the left and the right sides of the lattice are fixed occupied. The two columns of occupied sites at the ends form two initial clusters on the lattice. The interior of lattice is initially empty and as each site is added, a test is performed that reveals when the end clusters first become connected. The test is based on assigning a root site to each cluster and then labeling sites connected to the root sites. A connection between the root sites reveals that spanning has occurred.

A. Zero gradient

To compare to known percolation results, simulations were run up to $L = 8192$, so $N = L \times L$ has a maximum of 67 108 864 sites. Results for $\langle n_c\rangle$ as a function of L are shown in Fig. 4. In the limit $L \to \infty$ this gives an estimate of $\langle n_c\rangle = 0.592\,746(2)$, consistent with, but no better than, the best published estimates of the percolation threshold, such as 0.592 745 98(4), from Lee's [25] examination of

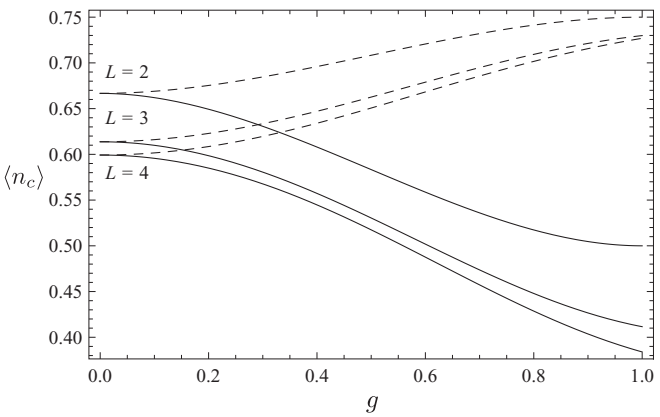

FIG. 2. Exact results for the mean spanning threshold on small two-dimensional networks. Solid lines are for spanning in the direction perpendicular to the gradient $\langle n_{c\perp}\rangle$ and dashed lines are for spanning in the direction of the gradient $\langle n_{c\parallel}\rangle$.

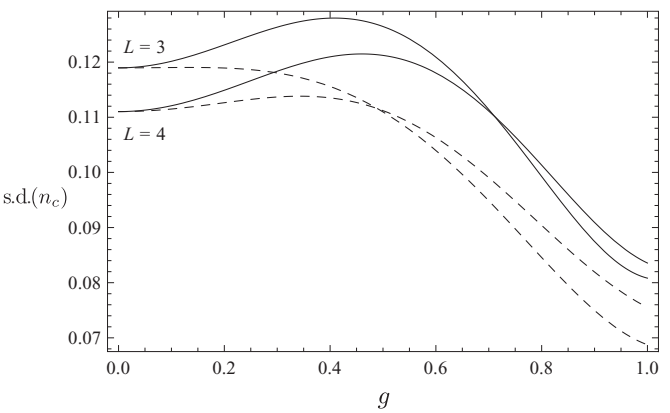

FIG. 3. Exact results for the standard deviation of the spanning threshold s.d.(n_c) on small two dimensional networks. Solid lines are for spanning in the direction perpendicular to the gradient and dashed lines are for spanning in the direction of the gradient.

TABLE III. Exact results for the variance of the spanning threshold in D dimensions with gradient g, $0 \leqslant g \leqslant 1$.

D	L	$\mathrm{Var}(n_{c\perp})$	$\mathrm{Var}(n_{c\parallel})$
2	2	$(-8g^6+24g^5-18g^4-2g^3+3g^2+1)/72$	$(-4g^6+12g^5-9g^4+2g^3-3g^2+2)/144$
2	3	$(-8649g^{14}+65100g^{13}+41552g^{12}-1359540g^{11}$ $+2015076g^{10}+8132768g^9-20055700g^8$ $-10741632g^7+50466640g^6-12971280g^5$ $-24075184g^4+6749120g^2+3235200)/228614400$	$(-4g^{18}+408g^{16}-3360g^{15}+3960g^{14}+145488g^{13}$ $-1438164g^{12}+7380864g^{11}-23761521g^{10}$ $+45021784g^9-29859984g^8-50201616g^7$ $+81993408g^6+15701280g^5-55418304g^4$ $+1816320g^2+12940800)/914457600$
2	4	$(-13006946304g^{30}+7427114145792g^{28}$ $-47345284546560g^{27}-958653042274368g^{26}$ $+1332140114777472 0g^{25}-717401703287168 64g^{24}$ $+242460188327708208g^{23}-65879551182589 5184g^{22}$ $+927009150376331880g^{21}+213762752643689 0631g^{20}$ $-949065101884580709 6g^{19}+752328138408487 6410g^{18}$ $+674796431372786078 4g^{17}-106691174820096005997g^{16}$ $+496658927106401991120g^{15}-136740337795656645336g^{14}$ $-244150356521684016734 4g^{13}+100553097122578328 8572g^{12}$ $+783153494678044119801 6g^{11}-738583696122174204588g^{10}$ $-159456731618022966167 04g^9-162018710590013268025 32g^8$ $+511258694607655222250 88g^7-151455740175936540835 92g^6$ $-161523927757282048358 4g^5-158859654285544175776 68g^4$ $+635722313974282355040 0g^2+321489149502202326651 6)/$ 260807895229592200089600	$(-278422596g^{30}-67812571440g^{28}$ $+319288545576g^{27}-5728826073096g^{26}$ $+42918240541176g^{25}-259198990809876g^{24}$ $+1155352080816648g^{23}-414277433684140g^{22}$ $-363814005376209 96g^{21}+318239988491833980g^{20}$ $-162450562327856758 8g^{19}+476190299721545838 0g^{18}$ $+789171699111023664g^{17}-865689474528595070 64g^{16}$ $+472886946938688112980g^{15}-147485919282341491 0512g^{14}$ $+299720864201626911 4452g^{13}-395028614842249115 9997g^{12}$ $+309888333666855656 8560g^{11}-127844903228602015 9422g^{10}$ $+842454944413231756464g^9-134267255833648316 6871g^8$ $+405110838320037495 36g^7+173855844907283349 3690g^6$ $-101144370468804062 4000g^5-176185795979806152 849g^4$ $+777778382481223701 60g^2+893025415283895351 81)/$ $724466375637756111 3600$
3	2	$(-32g^{14}+1792g^{12}-2240g^{11}-27328g^{10}$ $+66304g^9+23520g^8-176364g^7+86240g^6$ $+105616g^5-60872g^4-34020g^3+13272g^2$ $+5337)/352800$	$-(g-1)^2(4g^{12}+8g^{11}+124g^{10}+100g^9$ $+1140g^8-228g^7+3549g^6-3448g^5$ $+2295g^4-5990g^3-1346g^2-2372g$ $-1186)/78400$

pseudo-random-number generators in Monte Carlo studies of site percolation. While the method used here does not give the same accuracy for modest computer resources, this method gives results consistent with other methods of calculating the percolation threshold for uncorrelated networks, with the advantage that this method is easily adopted to provide results for lattices with a gradient.

It has been found that finite-size scaling of the standard error Δ goes as $\Delta \propto L^{-1/\nu}$, where ν is the correlation length exponent [26]. In two-dimensional uncorrelated percolation $\nu = 4/3 \approx 1.33$ [20], so $\Delta \propto L^{-0.75}$ is expected from the simulations. For the simulations reported here $\Delta^2 = \langle n_c^2\rangle - \langle n_c\rangle^2$, so $\Delta = 0.492L^{-0.740}$ was measured for $L \geqslant 256$ (see Fig. 5) and $\Delta = 0.514L^{-0.746}$ for $L \geqslant 1024$. These values are consistent with the expected number.

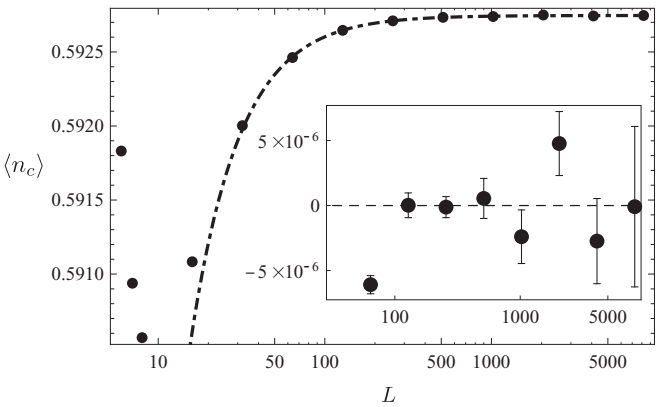

FIG. 4. Mean spanning threshold $\langle n_c\rangle$ as a function of network size L, on an uncorrelated square network. The dashed curve is the fit of $\langle n_c\rangle = a + bL^{-c}$ to the simulation points for $L \geqslant 128$ giving $a = 0.592\,746$, $b = -0.126$, and $c = 1.47$. The inset shows the difference between the points and the fitting curve, with the standard error shown by the bars.

B. With a gradient

Numerous simulations were run at a variety of values for g and L. Fitting the results for $\langle n_c\rangle$ with the function $a + bL^{-c}$ in the range $L \geqslant 1024$ gives the values for a, b, and c in Table IV.

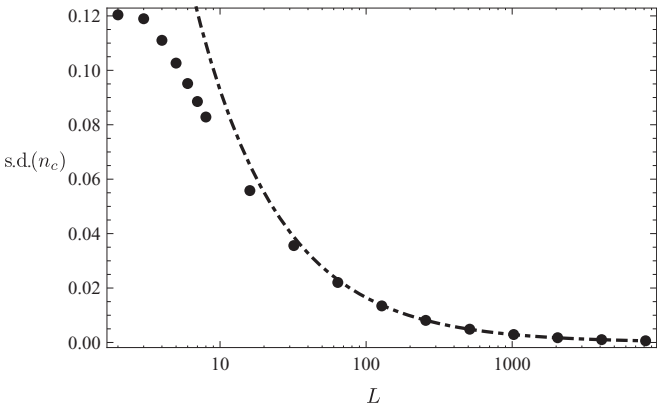

FIG. 5. Standard deviation in the spanning threshold n_c as a function of network size L, on an uncorrelated square network. The dashed curve is the fit to the points $L \geqslant 256$ giving $0.52L^{-0.75}$.

TABLE IV. Simulation results for $\langle n_c \rangle$ in two dimensions fitted to $a + bL^{-c}$ with $L \geqslant 1024$.

Gradient g	a	b	c
	Perpendicular $\perp$		
0.125	0.527	0.20	0.29
0.250	0.463	0.32	0.31
0.375	0.402	0.43	0.32
0.500	0.340	0.54	0.34
0.625	0.277	0.61	0.34
0.750	0.233	0.65	0.37
0.875	0.200	0.62	0.37
1.000	0.175	0.61	0.38
	Parallel $\parallel$		
0.125	0.659	−0.20	0.29
0.250	0.721	−0.34	0.32
0.375	0.784	−0.45	0.33
0.500	0.836	−0.55	0.36
0.625	0.869	−0.53	0.37
0.750	0.890	−0.52	0.38
0.875	0.906	−0.51	0.39
1.000	0.917	−0.50	0.40

Some examples of the results as a function of g are shown for $L = 512$ and $L = 4096$ in Fig. 6 and as a function of L for a gradient $g = 0.5$ in Fig. 7.

The extrapolated limits as $L \to \infty$ of the fitting curves for various values of g, both parallel and perpendicular, are shown as the dots in Fig. 8. These extrapolated limits are the values for a in Table IV. In Fig. 8 these numerical limits are compared to the following equations that would be expected from simple linear weighting of the site densities given by Eq. (1):

$$\langle n_{c\parallel} \rangle = p_c - \frac{g}{2}, \quad g \leqslant p_c \tag{9}$$

$$\langle n_{c\parallel} \rangle = \frac{p_c^2}{2g}, \quad g \geqslant p_c \tag{10}$$

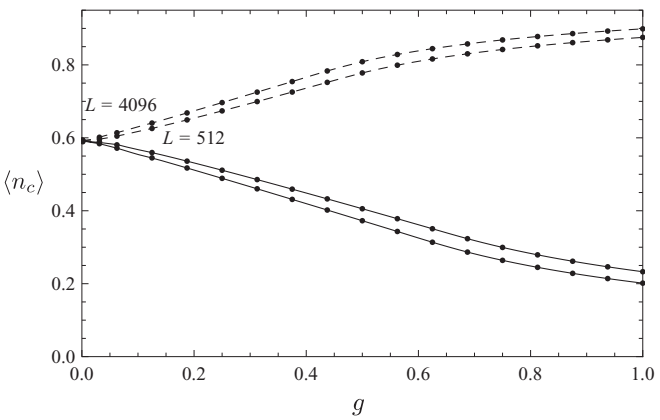

FIG. 6. Numerical estimates of the mean spanning threshold $\langle n_c \rangle$ as a function of the gradient g for $L = 512$ and 4096. Solid lines are for spanning in the direction perpendicular to the gradient, dashed lines are for spanning in the direction of the gradient, and small circles are points obtained from simulations.

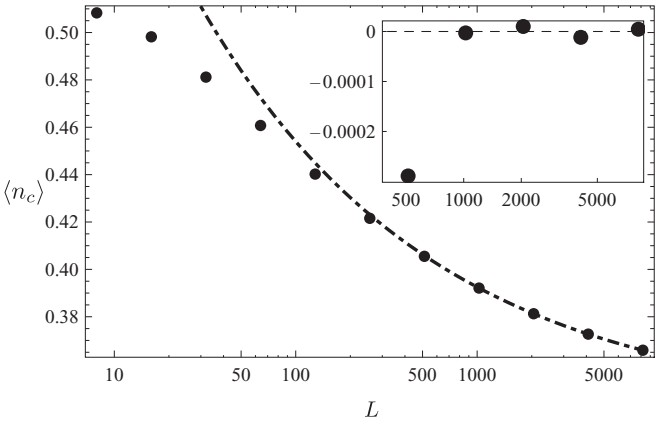

FIG. 7. Example of spanning thresholds perpendicular to the gradient $\langle n_{c\perp} \rangle$ as a function of L, for gradient $g = 0.5$. The fitting curves are used to extrapolate to $L \to \infty$. The inset shows the difference between the points and the fitting curve.

$$\langle n_{c\perp} \rangle = p_c + \frac{g}{2}, \quad g \leqslant 1 - p_c \tag{11}$$

$$\langle n_{c\perp} \rangle = 1 - \frac{(1-p_c)^2}{2g}, \quad g \geqslant 1 - p_c. \tag{12}$$

The change from a linear relationship occurs when the gradient is sufficiently steep that one edge has sites that cannot be occupied (for spanning perpendicular to the gradient) or are fully occupied (for spanning parallel to the gradient). Here, in two dimensions $p_c = \langle n_c \rangle \sim 0.592\,746$. With a gradient in the range $0.2 < g < 0.5$ the correlation length exponent appears to be around $\nu = 1.9$–2.0, significantly greater than two-dimensional uncorrelated percolation with $\nu = 4/3$.

Standard deviations of the spanning threshold as a function of g for $L = 512$ on a square network are shown in Fig. 9. The standard deviation of the spanning threshold perpendicular to the gradient reaches a maximum around $g = 0.66$. Similarly,

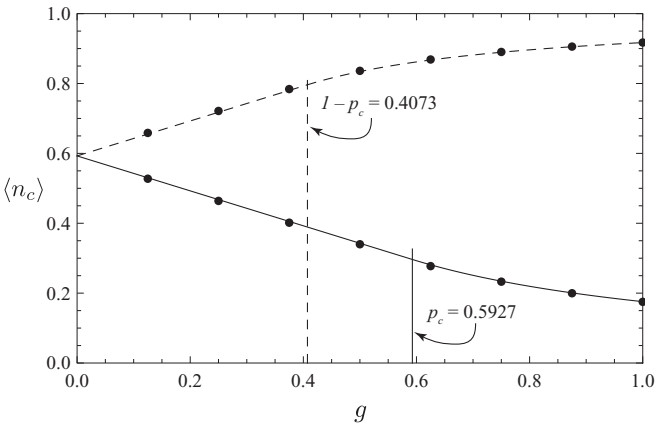

FIG. 8. Extrapolated limit as $L \to \infty$ of the spanning threshold in two dimensions. Dots are derived from the numerical simulations and the lines represent Eqs. (9)–(12). Solid lines are for spanning in the direction perpendicular to the gradient $\langle n_{c\perp} \rangle$ and dashed lines are for spanning parallel to the gradient $\langle n_{c\parallel} \rangle$.

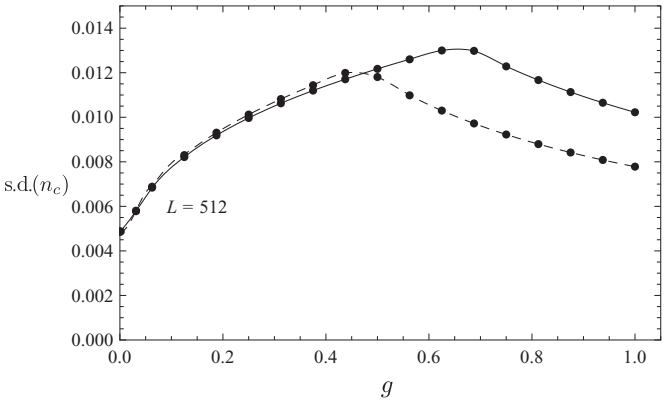

FIG. 9. Numerical result for the standard deviation of the spanning threshold s.d.(n_c) as a function of the gradient g on a square network with $L = 512$. Solid lines are for spanning in the direction perpendicular to the gradient and dashed lines are for spanning in the direction of the gradient.

the standard deviation for spanning perpendicular to the gradient has a maximum around $g = 0.47$.

IV. EXACT RESULTS IN THREE DIMENSIONS

A. Zero gradient

The same approach that was used in two dimensions can be applied to small $L \times L \times L$ networks in three dimensions. For $L = 2$ with $N = 8$, $\langle n_c \rangle$ is given by

$$(0,1/7,2/7,12/35,8/35,0,0,0) \times (1,2,3,4,5,6,7,8)/8, \quad (13)$$

so

$$\langle n_c \rangle = 16/35. \quad (14)$$

This result for $L = 2$ and the result for $L = 3$ are shown in Table V. The explosive growth in calculation effort with increasing L rapidly presents a barrier for determining the result for $L = 4$ ($N = 64$).

B. With a gradient

Exact solutions for $L = 2$ are in Table II and are plotted in Fig. 10 with standard deviations in Fig. 11.

V. NUMERICAL RESULTS IN THREE DIMENSIONS

A. Zero gradient

In three dimensions simulations were run up to $L = 384$, so $N = L \times L \times L = 56\,623\,104$ sites. Results for an uncorrelated network are shown in Fig. 12. In the limit $L \to \infty$ this gives an estimate of $\langle n_c \rangle = 0.311\,61(1)$, consistent with, but no better than, the best published estimates of the percolation

TABLE V. Exact results in three dimensions, with no gradient.

L	$\langle n_c \rangle$ exact fraction	$\langle n_c \rangle$ decimal fraction
2	16/35	0.45714286
3	385753183/992885850	0.38851715

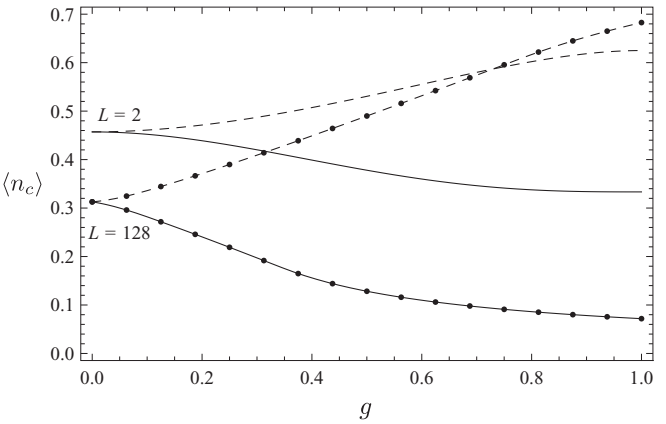

FIG. 10. Exact result for $L = 2$ and numerical result for $L = 128$ for the mean spanning threshold $\langle n_c \rangle$ as a function of the gradient g on a cubic network. Solid lines are for spanning in the direction perpendicular to the gradient and dashed lines are for spanning in the direction of the gradient.

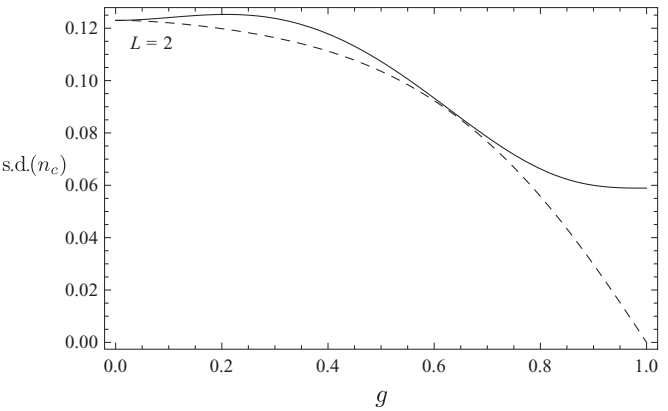

FIG. 11. Exact results for the standard deviation of the spanning threshold on a three-dimensional network with $L = 2$. Solid lines are for spanning in the direction perpendicular to the gradient and dashed lines are for spanning in the direction of the gradient.

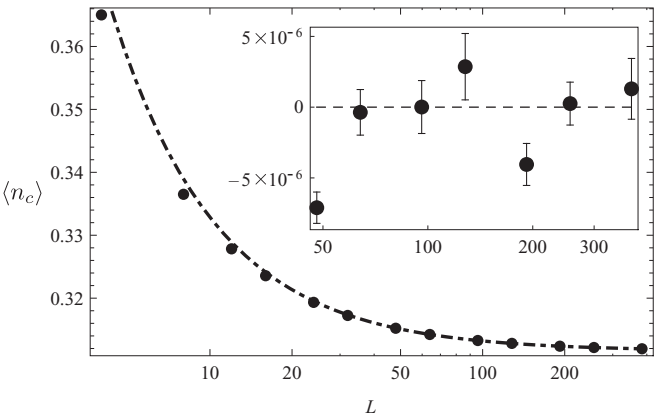

FIG. 12. Mean spanning threshold $\langle n_c \rangle$ as a function of network size L, on an uncorrelated cubic network, with $g = 0$. The dashed curve is the fit of $\langle n_c \rangle = a + bL^{-c}$ to the points $L \geqslant 96$ giving $a = 0.311\,61$, $b = 0.28$, and $c = 1.13$. The inset shows the difference between the points and the fitting curve, with the standard error shown by the bars.

TABLE VI. Simulation results for $\langle n_c \rangle$ in three dimensions fitted to $a + bL^{-c}$ with $L \geqslant 128$.

Gradient g	a	b	c
	Perpendicular $\perp$		
0.125	0.248	0.25	0.49
0.250	0.185	0.35	0.48
0.375	0.130	0.46	0.53
0.500	0.098	0.44	0.55
0.625	0.078	0.40	0.55
0.750	0.066	0.39	0.56
0.875	0.056	0.37	0.56
1.000	0.049	0.35	0.56
	Parallel $\parallel$		
0.125	0.384	−0.14	0.26
0.250	0.444	−0.26	0.32
0.375	0.507	−0.35	0.34
0.500	0.567	−0.44	0.36
0.625	0.637	−0.48	0.34
0.750	0.704	−0.52	0.33
0.875	0.744	−0.54	0.35
1.000	0.778	−0.52	0.35

threshold on a cubic network of $p_c = 0.311\,607\,7(3)$ [27] and $p_c = 0.311\,600\,4(35)$ [28]. Established values of the correlation length exponent for the three-dimensional site lattice are $\nu = 0.89$ [20] and $\nu = 0.88$ [26]; here the value $\nu = 1/1.13 = 0.89$ is obtained.

B. With a gradient

In three dimensions spanning can be considered in three directions. However, two of these directions are perpendicular to the gradient and so give identical results.

Numerous simulations were run at a variety of values for g and L. Fitting the results for $\langle n_c \rangle$ with the function $a + bL^{-c}$ in the range $L \geqslant 128$ gives the values for a, b, and c in Table VI. Some examples of the results as a function of L for gradients $g = 0.5$ for $n_{c\perp}(L)$ are shown in Fig. 13 and $n_{c\parallel}(L)$ in Fig. 14.

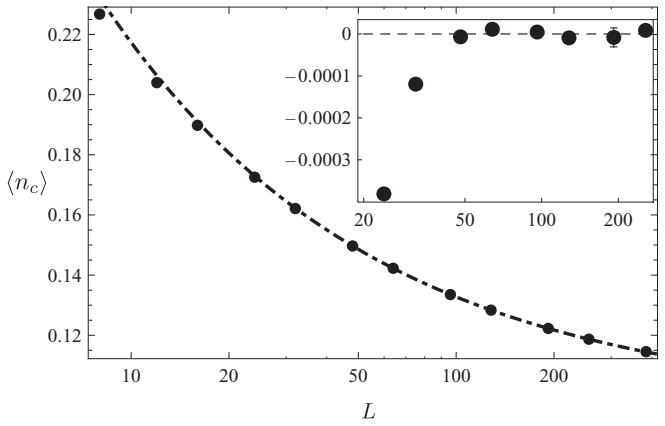

FIG. 13. Mean spanning threshold $n_{c\perp}(L)$ as a function of network size L, with gradient $g = 0.5$ on a cubic network. Also plotted is the relevant fitting curve from Table VI. The inset shows the difference between the points and the fitting curve.

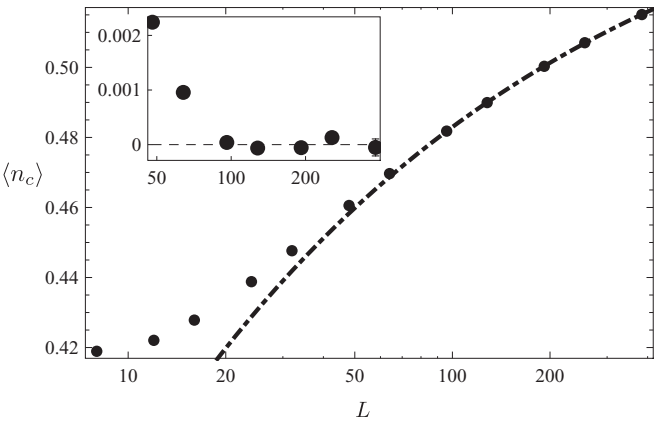

FIG. 14. Mean spanning threshold $n_{c\parallel}(L)$ as a function of network size L, with gradient $g = 0.5$ on a cubic network. Also plotted is the relevant fitting curve from Table VI. The inset shows the difference between the points and the fitting curve.

Standard deviations of the spanning threshold as a function of g for $L = 128$ on a cubic network are shown in Fig. 15. The standard deviation of the spanning threshold perpendicular to the gradient reaches a maximum around $g = 0.34$. Similarly, the standard deviation for spanning perpendicular to the gradient has a maximum at $g = 0.78$.

The extrapolated limits as $L \to \infty$ of the fitting curves for various values of g, both parallel and perpendicular, are shown as the dots in Fig. 16. These limits are compared to Eqs. (9)–(12). This is similar to the two-dimensional results, except that here in three dimensions $p_c \sim 0.311\,608$.

For finite L with an extremely large gradient

$$\langle n_{c\parallel 3D} \rangle = \frac{\langle n_{c2D} \rangle}{L}, \quad g \geqslant L, \tag{15}$$

where $\langle n_{c\parallel 3D} \rangle$ is the mean spanning threshold parallel to the gradient in three dimensions and $\langle n_{c2D} \rangle$ is the mean spanning threshold for no gradient ($g = 0$) in two dimensions. This situation is when only sites on one face are becoming occupied, so it essentially reduces to two-dimensional percolation.

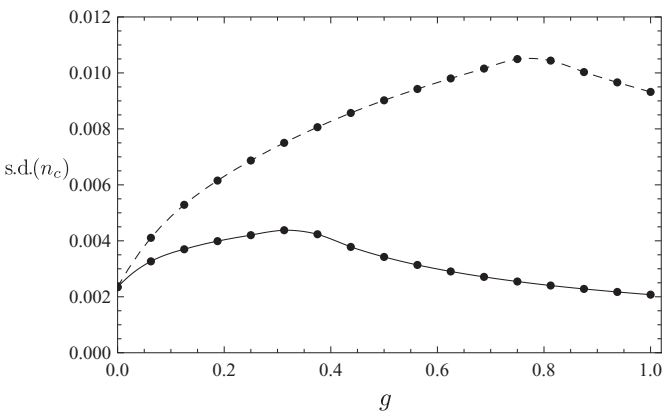

FIG. 15. Standard deviation of the spanning threshold as a function of g for $L = 128$ on a cubic network. Solid lines are for spanning in the direction perpendicular to the gradient and dashed lines are for spanning in the direction of the gradient.

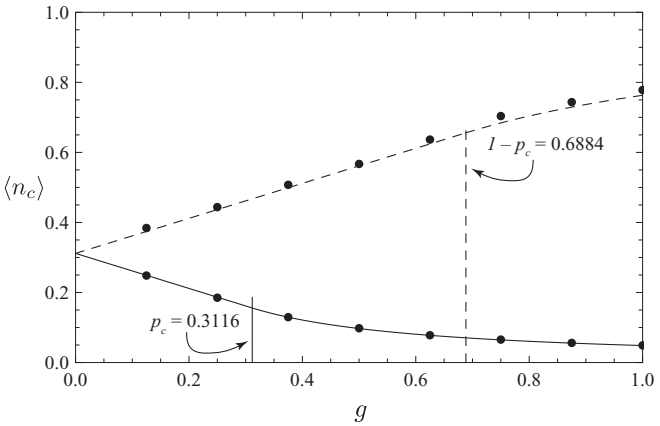

FIG. 16. Extrapolated limit of the spanning threshold in three dimensions. Dots are derived from the numerical simulations and the lines represent Eqs. (9)–(12). Solid lines are for spanning in the direction perpendicular to the gradient $\langle n_{c\perp}\rangle$ and dashed lines are for spanning parallel to the gradient $\langle n_{c\parallel}\rangle$.

VI. DISCUSSION

There is the opportunity to reflect here on potential future studies. While the current study has been limited to ordinary site percolation, further similar studies more relevant to the physics of fluid trapping could be undertaken using models such as percolation with trapping [29,30], although this requires additional computational effort. Indeed, ordinary percolation and percolation with trapping can give similar results. Ultimately, predictive modeling of real porous media requires a more complex models of the pore space [31].

Recent years have seen rapid development in x-ray microtomography as a technique to measure the pore space of rocks and characterize fluid residual trapping [32–35]. The rock types that have received the most attention are relatively homogeneous and isotropic as these are most easily interpreted, but it should be possible to measure the effective gradient in pore properties for cores that display upward coarsening or upward fining. This would provide g values for relevant rocks that could be deployed in network models.

Furthermore, it would be possible to extend this study to consider functions other than the linear equation (1) for the site occupancy. With another function, such as through replacing g by g^2, a set of equations different from but related to Eqs. (9)–(12) could be derived.

VII. CONCLUSION

The extrapolated limits of the mean spanning threshold $\langle n_c\rangle$ as $L \to \infty$ for site percolation with a gradient have been verified to be given by Eqs. (9)–(12) in both two and three dimensions. Although not surprising, this straightforward linear dependence on gradient for moderate gradients is a useful result. It means that results for other forms of heterogeneity can easily be obtained if the site occupancy can be expressed as a combination of piecewise linear gradient combinations.

This study has also addressed finite-size scaling. Exact small network solutions have been provided for $L \leqslant 4$ in two dimensions and $L = 2$ in three dimensions. Exact solutions with $L > 4$ in two dimensions and $L > 2$ in three dimensions may be possible with more complete use of symmetry and larger computational resources, but the explosive growth in calculation time with increasing L presents a barrier.

[1] M. Sahimi, Long-range correlated percolation and flow and transport in heterogeneous porous media, J. Phys. I France **4**, 1263 (1994).
[2] M. Sahimi and S. Mukhopadhyay, Scaling properties of a percolation model with long-range correlations, Phys. Rev. E **54**, 3870 (1996).
[3] C. Du, C. Satik, and Y. C. Yortsos, Percolation in a fractional Brownian motion lattice, AIChE J. **42**, 2392 (1996).
[4] L. Paterson, S. Painter, M. A. Knackstedt, and W. V. Pinczewski, Patterns of fluid flow in naturally heterogeneous rocks, Physica A **233**, 619 (1996).
[5] L. Paterson, S. Painter, X. Zhang, and W. V. Pinczewski, Simulating residual saturation and relative permeability in heterogeneous formations, SPE J. **3**, 211 (1998).
[6] M. A. Knackstedt, M. Sahimi, and A. P. Sheppard, Invasion percolation with long-range correlations: First-order phase transition and nonuniversal scaling properties, Phys. Rev. E **61**, 4920 (2000).
[7] S. J. Marrink, L. Paterson, and M. A. Knackstedt, Definition of percolation thresholds on self-affine surfaces, Physica A **280**, 207 (2000).
[8] M. Hohn, *Geostatistics and Petroleum Geology*, 2nd ed. (Kluwer, Dordrecht, 1999).
[9] B. Sapoval, M. Rosso, and J.-F. Gouyet, The fractal nature of a diffusion front and the relation to percolation, J. Phys. Lett. Paris **46**, 149 (1985).
[10] D. Wilkinson, Percolation model of immiscible displacement in the presence of buoyancy forces, Phys. Rev. A **30**, 520 (1984).
[11] R. M. Ziff and B. Sapoval, The efficient determination of the percolation threshold by a frontier-generating walk in a gradient, J. Phys. A: Math. Gen. **19**, L1169 (1986).
[12] M. Rosso, J. F. Gouyet, and B. Sapoval, Gradient percolation in three dimensions and relation to diffusion fronts, Phys. Rev. Lett. **57**, 3195 (1986).
[13] A. Hansen, G. G. Batrouni, T. Ramstad, and J. Schmittbuhl, Self-affinity in the gradient percolation problem, Phys. Rev. E **75**, 030102 (2007).
[14] P. Nolin, Critical exponents of planar gradient percolation, Ann. Probab. **36**, 1748 (2008).
[15] M. T. Gastner and B. Oborny, The geometry of percolation fronts in two-dimensional lattices with spatially varying densities, New J. Phys. **14**, 103019 (2012).
[16] S. Roux, A. Hansen, and E. L. Hinrichsen, Percolation in a gradient: Conductivity properties, J. Phys. A: Math. Gen. **23**, L1253 (1990).

[17] J.-F. Gouyet and M. Rosso, Diffusion fronts and gradient percolation: A survey, Physica A **357**, 86 (2005).
[18] M. Chaouche, N. Rakotomalala, D. Salin, B. Xu, and Y. C. Yortsos, Invasion percolation in a hydrostatic or permeability gradient: Experiments and simulations, Phys. Rev. E **49**, 4133 (1994).
[19] T. Mulder and J. Alexander, The physical character of subaqueous sedimentary density flows and their deposits, Sedimentology **48**, 269 (2001).
[20] B. D. Hughes, *Random Walks and Random Environments* (Clarendon, Oxford, 1996), Vol. 2.
[21] R. M. Ziff and M. E. J. Newman, Convergence of threshold estimates for two-dimensional percolation, Phys. Rev. E **66**, 016129 (2002).
[22] M. E. J. Newman and R. M. Ziff, Efficient Monte Carlo algorithm and high-precision results for percolation, Phys. Rev. Lett. **85**, 4104 (2000).
[23] M. E. J. Newman and R. M. Ziff, Fast Monte Carlo algorithm for site or bond percolation, Phys. Rev. E **64**, 016706 (2001).
[24] See Supplemental Material at http://link.aps.org/supplemental/10.1103/PhysRevE.91.022116 for details of modifications to the Newman-Ziff algorithm used in this study.
[25] M. J. Lee, Pseudo-random-number generators and the square site percolation threshold, Phys. Rev. E **78**, 031131 (2008).
[26] D. Stauffer and A. Aharony, *Introduction to Percolation Theory*, 2nd ed. (Taylor & Francis, London, 1994).
[27] Y. Deng and H. W. J. Blöte, Monte Carlo study of the site-percolation model in two and three dimensions, Phys. Rev. E **72**, 016126 (2005).
[28] J. Škvor and I. Nezbeda, Percolation threshold parameters of fluids, Phys. Rev. E **79**, 041141 (2009).
[29] L. Paterson, Trapping thresholds in ordinary site percolation, Phys. Rev. E **58**, 7137 (1998).
[30] L. Paterson, A. P. Sheppard, and M. A. Knackstedt, Trapping thresholds in invasion percolation, Phys. Rev. E **66**, 056122 (2002).
[31] M. J. Blunt, Flow in porous media–pore-network models and multiphase flow, Curr. Opin. Colloid Interface Sci. **6**, 197 (2001).
[32] H. Dong and M. J. Blunt, Pore-network extraction from micro-computerized-tomography images, Phys. Rev. E **80**, 036307 (2009).
[33] M. Kumar, T. Senden, M. A. Knackstedt, S. J. Latham, V. Pinczewski, R. M. Sok, A. P. Sheppard, and M. L. Turner, Imaging of pore scale distribution of fluids and wettability, Petrophysics **50**, 311 (2009).
[34] S. Iglauer, S. Favretto, G. Spinelli, G. Schena, and M. J. Blunt, X-ray tomography measurements of power-law cluster size distributions for the nonwetting phase in sandstones, Phys. Rev. E **82**, 056315 (2010).
[35] Y. Tanino and M. J. Blunt, Capillary trapping in sandstones and carbonates: Dependence on pore structure, Water Resour. Res. **48**, W08525 (2012).